

Measurement of the Hall Dynamo Effect during Magnetic Reconnection in a High-Temperature Plasma

W. X. Ding,^{1,3} D. L. Brower,^{1,3} D. Craig,^{2,3} B. H. Deng,^{1,3} G. Fiksel,^{2,3} V. Mirnov,^{2,3} S. C. Prager,^{2,3}
J. S. Sarff,^{2,3} and V. Svidzinski^{2,3}

¹*Electrical Engineering Department, University of California at Los Angeles, Los Angeles, California 90095, USA*

²*Physics Department, University of Wisconsin-Madison, Madison, Wisconsin 53706, USA*

³*Center for Magnetic Self-Organization in Astrophysical and Laboratory Plasmas, University of Wisconsin-Madison, Madison, Wisconsin 53706, USA*

(Received 4 March 2004; published 20 July 2004)

The fluctuation-induced Hall electromotive force, $\langle \delta \vec{J} \times \delta \vec{B} \rangle / n_e e$, is experimentally measured in the high-temperature interior of a reversed-field pinch plasma by a fast Faraday rotation diagnostic. It is found that the Hall dynamo effect is significant, redistributing (flattening) the equilibrium core current near the resonant surface during a reconnection event. These results imply that effects beyond single-fluid MHD are important for the dynamo and magnetic reconnection.

DOI: 10.1103/PhysRevLett.93.045002

PACS numbers: 52.25.Gj, 52.35.Py, 52.35.Vd, 52.55.Hc

Magnetic reconnection and self-generation of magnetic field are two coupled processes widespread in both laboratory and astrophysical plasmas. Many explanations for magnetic field generation, the dynamo effect, rely upon the simultaneous occurrence of reconnection. Over the past several decades the dynamo has been treated mainly as a single-fluid MHD phenomenon. However, there are also processes beyond MHD that can produce dynamo effects. In this Letter, we present experimental observation of the Hall dynamo—a dynamo effect that arises from the Hall term in two-fluid theory. The observations also establish the importance of the two-fluid Hall effect in magnetic reconnection (or plasma relaxation [1]).

The two-fluid physics of dynamo and reconnection is captured by generalized Ohm's law [2]

$$-\frac{m_e}{e^2 n_e} \frac{\partial \vec{J}}{\partial t} + \vec{E} + \vec{v} \times \vec{B} - \frac{1}{n_e e} \vec{J} \times \vec{B} + \frac{\nabla P_e}{n_e e} = \eta \vec{J}, \quad (1)$$

where n_e is the electron density, e is electron charge, and P_e is electron pressure. J , E , v , B , η are the plasma current density, electric field, ion velocity, magnetic field, and resistivity. Both reconnection and dynamo are generated by spatial (and possibly temporal) fluctuations in the various fields contained in the two-fluid description. The parallel mean-field Ohm's law is constructed to isolate the different dynamo mechanisms. We decompose each quantity into mean and fluctuating parts, and take the ensemble average of the parallel component of Eq. (1) to yield

$$\langle E \rangle_{\parallel} + \langle \delta \vec{v} \times \delta \vec{B} \rangle_{\parallel} - \langle \delta \vec{J} \times \delta \vec{B} \rangle_{\parallel} / n_e e = \eta_{\parallel} \langle J_{\parallel} \rangle, \quad (2)$$

where δ denotes a fluctuating quantity, $\langle \rangle$ denotes a mean or ensemble-averaged quantity, the inertial term (dJ/dt) is negligible, and all other quadratic terms driven by density and electron pressure fluctuations vanish upon ensemble averaging. We note that mean current (right-hand side) can be driven by two fluctuation-induced

terms: the MHD dynamo (second term on left-hand side) arising from the correlation of magnetic and velocity fluctuations, and the Hall dynamo (third term) arising from the correlation of the magnetic and current density fluctuations.

In the reversed-field pinch (RFP) laboratory plasma, the current profile undergoes a sawtooth (or relaxation) oscillation characterized by a slow peaking of current profile followed by a rapid flattening. It is well known that during a plasma relaxation event the current density is not balanced by the electric field (first term on the left-hand side). During relaxation, corresponding to the crash phase of a sawtooth oscillation, the current density profile is altered by fluctuations arising from tearing instabilities. Nonlinear MHD theory provides a detailed explanation for the current profile relaxation based on the MHD dynamo [1,3]. However, recent analytical, quasi-linear calculation suggests that the Hall dynamo may be important [4]. Computation of Hall dynamo for astrophysical application [5] and laboratory plasma [6] also indicates that there are situations where the Hall dynamo could be significant.

We report here measurements of the Hall dynamo in the Madison Symmetric Torus (MST) RFP experiment. Prior measurements in the extreme edge of MST (the outer 10%, beyond the reversal surface) with probes have shown that the MHD dynamo is strong [7], while the Hall dynamo is weak [8]. However, it was also observed that the MHD dynamo becomes weak for deeper probe insertion. We have now measured the magnetic field and current density fluctuations (and their spatial distribution) in the hot plasma core using a high-speed laser Faraday rotation diagnostic. We find that the Hall dynamo is significant and acts to reduce the core mean current during a sawtooth crash when the current density profile relaxes toward a minimum energy state. These results indicate that effects beyond single-fluid MHD may be important for the dynamo and reconnection.

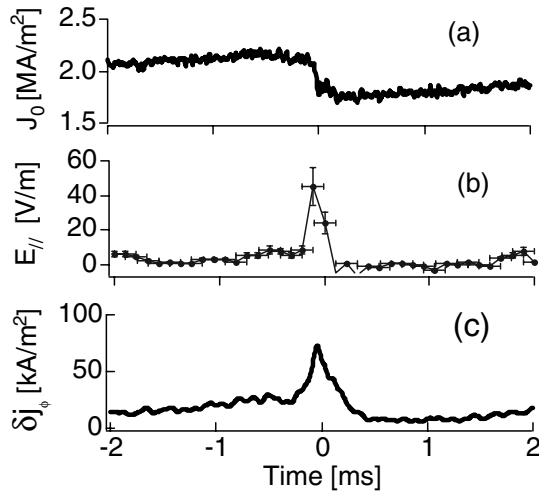


FIG. 1. Dynamics of (a) equilibrium current density at the magnetic axis, (b) inductive equilibrium electric field, and (c) local current density fluctuation near the resonant surface for (1, 6) mode during plasma relaxation event (sawtooth crash).

MST is a device with major radius $R_0 = 1.5$ m, minor radius $a = 0.52$ m, discharge current $350 \sim 400$ kA, line-averaged electron density $\bar{n}_e \sim 1 \times 10^{19} \text{ m}^{-3}$, and electron temperature $T_{eo} \sim 300$ eV. MST plasma is confined by the toroidal magnetic field B_{ϕ} and comparable poloidal magnetic field B_{θ} . Safety factor $q(r) = \frac{r}{R_0} [B_{\phi}(r)/B_{\theta}(r)] \leq 0.2$ on the magnetic axis and monotonically decreases toward plasma edge where it reverses sign. Magnetic fluctuations in MST have a broad spectrum but are dominated by core resonant tearing modes with poloidal, toroidal mode numbers $m = 1, n = 5-10$, respectively. Typically, the core resonant (1, 6) mode has the largest amplitude and will be the focus of this Letter.

$$\frac{\langle \delta \vec{J} \times \delta \vec{B} \rangle}{n_e e} \cdot \frac{\vec{B}}{B} = \frac{A_1}{n_e e} \left\langle \left(\frac{1}{r} \frac{\partial}{\partial r} r \delta b_{\theta} \right) \delta b_r \right\rangle + \frac{A_2}{n_e e} \left\langle \frac{1}{r} \delta b_{\theta} \frac{\partial}{\partial r} r \delta b_r \right\rangle = A_1 \frac{\langle \delta j_{\phi} \delta b_r \rangle}{n_e e} + \frac{A_2}{n_e e} \left\langle \frac{1}{r} \delta b_{\theta} \frac{\partial}{\partial r} r \delta b_r \right\rangle \approx A_1 \frac{\langle \delta j_{\phi} \delta b_r \rangle}{n_e e}, \quad (4)$$

where

$$A_1 = \frac{B_{\theta}}{B} \left[1 + \left(\frac{mR}{nr_s} \right)^2 \right] = \frac{B_{\theta}}{B} \left[1 + \left(\frac{B_{\phi}}{B_{\theta}} \right)^2 \right],$$

$$A_2 = \frac{B_{\theta}}{B} \left[1 - \left(\frac{mR}{nr_s} \right)^2 \right] = \frac{B_{\theta}}{B} \left[1 - \left(\frac{B_{\phi}}{B_{\theta}} \right)^2 \right]$$

and B_{ϕ} , B_{θ} , and B are the known equilibrium toroidal, poloidal and total magnetic field. The $\left\langle \frac{1}{r} \delta b_{\theta} \frac{\partial}{\partial r} r \delta b_r \right\rangle$ term is found to be small in experiments where $\delta b_{\theta}(r_s) \sim 0$ and $B_{\phi} \geq B_{\theta}$ near the resonant surface as will be discussed later.

To investigate the role of the Hall dynamo ($\langle \delta \vec{J} \times \delta \vec{B} \rangle_{||} / n_e e$) on the mean current density profile, we require measurement of (1) the local current density fluctuation, δj_{ϕ} (2) magnetic field fluctuation δb_r , and (3) their

Magnetic field, magnetic field fluctuations, and current density fluctuations are measured by a fast (up to $\sim 1 \mu\text{s}$) Faraday rotation diagnostic [9] where 11 chords (chord separation ~ 8 cm) probe the plasma cross section vertically. MST discharges display a sawtooth cycle in many parameters. Prompt reduction of the current density J_0 at the magnetic axis during a typical plasma relaxation event is shown in Fig. 1(a). All measured quantities in parallel Ohm's law are ensemble averaged over these reproducible sawtooth events. The induced toroidal electric field during relaxation is shown in Fig. 1(b), where $E_{\phi} \approx E_{||}$ for plasma core. This electric field is given by

$$E_{\phi}(r) = \frac{V_L}{2\pi R} - \int_r^a \frac{\partial}{\partial t} B_{\theta}(r') dr, \quad (3)$$

where V_L is the loop voltage measured at the plasma surface and the second term is obtained by measurement of equilibrium dynamics [10]. The current density profile changes much faster ($\sim 100-200 \mu\text{s}$) than a resistive diffusion time in the island [$\tau_R \sim \mu_0(w/\pi)^2/\eta \sim 160$ ms, where w is island width]. The induced electric field force is much greater than the collision force (ηJ , where $\eta \sim 2 \sim 4 \times 10^{-7} \Omega \text{ m}^{-1}$). A magnetic fluctuation-induced electromotive force is believed necessary to balance Ohm's Law and redistribute the mean current during the relaxation event.

In cylindrical coordinates, the Hall dynamo expression $\langle \delta \vec{J} \times \delta \vec{B} \rangle_{||} / n_e e$ can be rewritten by using $\nabla \cdot \delta \vec{B} = 0$, $\nabla \times \delta \vec{B} = \mu_0 \delta \vec{J}$, and taking a flux surface average of the fluctuations where $\langle i \delta b_l \delta b_l \rangle = (1/4\pi^2) \int_0^{2\pi} \int_0^{2\pi} i \delta b_l \delta b_l d\theta d\phi = 0, l = r, \theta, \phi$. This results in a simplified expression for the parallel component of the Hall dynamo in terms of $(\delta b_r, \delta b_{\theta})$ near the resonant surface ($\vec{k} \cdot \vec{B} = \frac{m}{r} B_{\theta} + \frac{n}{R} B_{\phi} = 0$):

correlation. In the following, each of these measurements will be discussed.

First, current density fluctuations are measured directly by Faraday rotation. It has previously been established [11] that the current fluctuation between polarimeter chords is

$$\delta I_{\phi} \approx \left(\int_{x_1} \delta \vec{B} \cdot d\vec{l} - \int_{x_2} \delta \vec{B} \cdot d\vec{l} \right) / \mu_0 = \Delta \tilde{\psi} / c_F \bar{n}_e \mu_0, \quad (5)$$

where c_F is a constant, $\tilde{\psi} = c_F \int n_e \delta \vec{B} \cdot d\vec{l} \approx c_F \bar{n}_e \int \delta \vec{B} \cdot d\vec{l}$ is the fluctuating Faraday rotation signal, x_1, x_2 are impact parameters of the selected chord pair, and \bar{n}_e is mean electron density. The above equation holds true for the central six polarimeter chords where the density fluctuations are negligible due to the small

density gradient in the core and the $m = 1$ nature of the perturbation [11,12]. This line-averaged measure of the current fluctuation (δI) can then be inverted to obtain the local current density perturbation, $\delta j_\phi(r)$ by asymmetric Abel inversion [12,13]. Since the measured helical current fluctuation is localized near the resonant surface $q = 1/6$ ($\vec{k} \cdot \vec{B}_0 = 0$), the temporal dynamics of the local current density fluctuation δj_ϕ can be directly measured by the pair of chords nearest the resonant surface, as shown in Fig. 1(c) for (1,6) mode. Using this approach, it is determined that the current density fluctuation amplitude reaches $\delta j_\phi/J_0 \sim 5\text{--}6\%$ at the sawtooth crash with radial extension ≤ 8 cm.

Second, the magnetic fluctuation amplitude spatial profile can be obtained by integrating the current fluctuation. However, in order to determine more precisely the magnetic and current density fluctuation profiles, we have developed a simple fitting routine where it is assumed that the resonant current density fluctuation profile has the form $\delta j_\phi(r) = j_a \exp\{-[(r - r_s)/w]^2\}$, with j_a (amplitude), r_s (resonant surface location), and w (width) serving as free parameters. Each is determined by making a best fit to the measured fluctuating Faraday rotation profiles. Once the fluctuating current density distribution is identified, the magnetic fluctuation spatial profile can be obtained by using $\nabla \times \delta B = \mu_0 \delta J$, $\nabla \cdot \delta B = 0$, and $\nabla \cdot \delta J = 0$ in a cylindrical geometry. Determination of the magnetic fluctuation spatial profile for a specific mode (m, n) is accomplished by integrating above equations with assumption $\delta j_\perp \ll \delta j_\parallel$ and boundary condition $\delta b_r(a) = 0$. Therefore, a modeled Faraday rotation fluctuation for a specified current profile $\tilde{\psi}^M(j_a, r_s, w) = c_F \int n_e(r) (\delta b_r \sin\theta + \delta b_\theta \cos\theta) dz$ can be constructed for each chord by minimizing $\chi^2 = \sum_{i=1}^6 \{[\tilde{\psi}_i - \tilde{\psi}_i^M(j_a, r_s, w)]^2 / \sigma_i^2\} + \{[\delta b_\theta^M(a) - b_\theta(a)]^2 / \sigma^2\}$ with respect to the free parameters (j_a, r_s , and w). For this expression, σ_i, σ are measurement error, $b_\theta(a)$ is measured by magnetic coils mounted inside the vessel, and $b_\theta^M(a)$ is a modeled value. In the minimization procedure we specify j_a, r_s, w and obtain both the magnetic field and current density fluctuation profiles. The measured Faraday rotation fluctuation profile and best fit result are shown in Fig. 2 for the (1,6) mode. Further details of the analysis procedure will be published elsewhere.

The resulting magnetic field fluctuation and current density fluctuation spatial profiles for the dominant, core resonant, (1,6) mode are shown in Fig. 3. Uncertainty due to the fitting procedure and experimental error is also estimated. Radial magnetic field fluctuations are observed to extend continuously through the rational surface indicating their resistive nature. Poloidal magnetic fluctuations change sign across the resonant surface, which is in qualitative agreement with previous measurements by probes in OHTE and ZT-40 [14] and MHD computation (DEBS code) [3]. A maximum in the current density fluctuation ($\delta j_\phi/J_0 \sim 4.5\%$) occurs at $r_s = 17$ cm where the (1,6) mode resonant surface is located

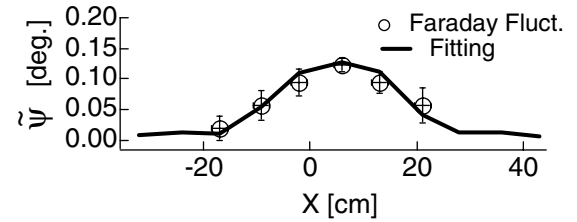


FIG. 2. Faraday rotation fluctuation amplitude for different chords for (1,6) mode. Circles represent measured Faraday rotation fluctuation. Solid line is fitting result.

based on equilibrium magnetic field measurements. The fluctuating current channel radial width is approximately 8 ± 3 cm. Amplitude, radial width and location are all consistent with the direct current density fluctuation measurement discussed earlier. Near the resonant surface, measurements show $\delta b_\theta(r_s) \sim 0$, $(\partial b_r / \partial r) \ll (\partial b_\theta / \partial r)$, and $B_\phi \geq B_\theta$, justifying the simplification made in Eq. (4).

Although the radial structure is localized, the $m = 1$ perturbation is distributed poloidally over a large region making the mode global. For a global mode, the multiple polarimeter chords can be used to spatially resolve the perturbed current profile. The current sheet width is much greater than the resistive skin depth (~ 0.2 cm) and is comparable to the ion skin depth (c/ω_{pi}) ~ 10 cm in MST where ω_{pi} is ion plasma frequency. Therefore, magnetic reconnection associated with mean current transport in MST occurs much faster than a resistive time. The measured fluctuation profiles are consistent with tearing mode theory where the current perturbation is local and the magnetic fluctuation is global.

Finally, the phase between δj_ϕ and δb_r can be obtained by ensemble averaging. In MST, rotation of the low- n magnetic modes transfers their spatial structure in the plasma frame into a temporal evolution in the lab frame. Since the magnetic modes are global, for convenience we correlate δj_ϕ to the specific helical magnetic mode which is spatially Fourier decomposed from 32 wall-mounted magnetic coils. After averaging over an ensemble of similar events, we can determine the phase between

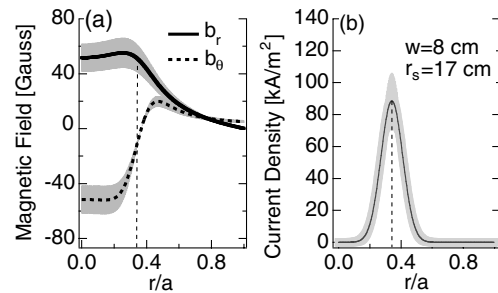


FIG. 3. (a) Radial and poloidal magnetic fluctuation spatial profile for dominant (1,6) mode, (b) corresponding current density fluctuation spatial profile. Vertical dashed line indicates (1,6) mode resonant surface.

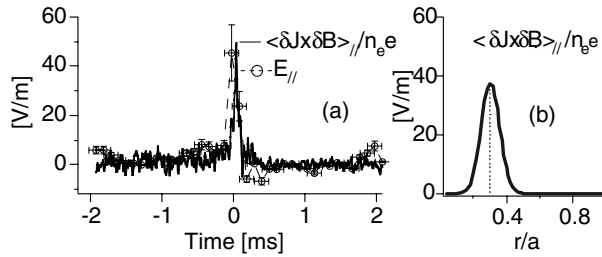


FIG. 4. (a) Dynamics of Hall dynamo (solid line) and inductive electric field (dashed line) during magnetic relaxation ($t = 0$ denotes sawtooth crash). (b) Hall dynamo spatial profile for (1,6) mode. Data ensemble averaged over 380 sawtooth events. Vertical dashed line indicates resonant surface.

$\delta j_{\phi}(r_s)$ and δb_r for the specified mode. For tearing modes, the perpendicular magnetic perturbation has a constant phase over minor radius [3,4], which has been verified by probe measurements in lower temperature plasmas. The measured Hall dynamo increases dramatically prior to the sawtooth crash, reaching $\sim 50 \pm 10$ V/m as shown by the solid line in Fig. 4. This occurs because the phase difference between the fluctuating current and magnetic field deviates from 90° (by 10°) while their amplitudes increase. Away from the sawtooth crash, the Hall electric field (averaged over time window -2 to -1 ms) is relatively small ($\sim 1.75 \pm 0.5$ V/m). At this time, the current density fluctuation has a near 90° phase difference with the magnetic fluctuations, although both δj_{ϕ} and δb_r are nonzero.

The Hall dynamo driven current in the core is found to oppose the mean current. From Fig. 4(a) it is observed that the large Hall electromotive force is comparable to the induced electric field and acts to suppress equilibrium current during plasma relaxation. The resistive force, ηJ , is small compared to both the induced electric field and the Hall dynamo during the sawtooth crash. This direct measurement of a substantial Hall dynamo in a high-temperature laboratory plasma indicates that two fluid effects are necessary to understand plasma relaxation.

The fluctuating current δj_{ϕ} peaks at the resonant surface and hence the Hall dynamo has a maximum there as well. As shown in Fig. 4(b), the width is ~ 8 cm. This is estimated by using Eq. (4) and assuming the current fluctuation phase is spatially constant. The Hall dynamo is spatially localized to the region of the resonant surface and an additional dynamo mechanism may be required to balance the induced electric field elsewhere. Such a picture is *qualitatively* consistent with quasilinear theory [4] which predicts a localized Hall dynamo and a more diffuse MHD dynamo away from the resonant surface. However, the measured width is much greater than that predicted. This implies that magnetic field fluctuation nonlinear dynamics play an important role in Hall dynamo. The relative contributions of different dynamo mechanisms (e.g., the Hall and MHD dynamo) across

the whole plasma cross section remains to be determined by future experiments.

The Hall dynamo on MST appears to be strongly influenced by nonlinear mode-mode interaction within a broad mode spectra in the RFP [e.g., coupling between (1,6), (1,7), and (0,1) modes] [1]. The nonlinear coupling of modes primarily alters the phase relation between fluctuating current and fluctuating magnetic field. In non-reversed plasma discharges where the $m = 0$ resonant surface is removed, we find the Hall dynamo decreases significantly, suggesting nonlinear mode coupling is indeed important.

In summary, we have measured the current density fluctuation and magnetic field fluctuation spatial profile in a high-temperature plasma by using a fast laser-based Faraday rotation diagnostic. These fluctuations have characteristics consistent with expectations for resistive tearing modes. The Hall electromotive force along the mean magnetic field direction, $\langle \delta \mathbf{j} \times \delta \mathbf{B} \rangle_{\parallel} / n_e e$, is found to be significant near the mode resonant surface. The Hall dynamo acts to reduce mean current density in the core and balances the inductive electric field induced at a sawtooth crash. These experiments establish that effects beyond single-fluid MHD are important for the dynamo and magnetic reconnection.

This work is supported by the U.S. Department of Energy.

-
- [1] S. Ortolani and D. D. Schnack, *Magnetohydrodynamics of Plasma Relaxation* (World Scientific, Singapore, 1993).
 - [2] L. Spitzer, Jr., *Physics of Fully Ionized Gases* (Interscience Publishers, New York, 1962), 2nd revised ed., p. 28.
 - [3] E. J. Caramana, R. A. Nebel, and D. D. Schnack, *Phys. Fluids* (1958–1988) **26**, 1305 (1983); Y. L. Ho and G. G. Graddock, *Phys. Fluids B* **3**, 721 (1991); A. Nagata *et al.*, *Phys. Fluids B* **3**, 1263 (1993).
 - [4] V. V. Mirnov, C. C. Hegna, and S. C. Prager, *Plasma Phys. Rep.* **29**, 612 (2003).
 - [5] P. D. Mininni, D. O. Gomez, and S. M. Mahajan, *Astrophys. J.* **587**, 472 (2003).
 - [6] R. A. Nebel, in *Proceedings of the Workshop on Physics of Alternative Magnetic Confinement Schemes, Varenna, Italy, 1990* (Italy Physics Society, Bologna, 1991), p. 611.
 - [7] P. W. Fontana *et al.*, *Phys. Rev. Lett.* **85**, 566 (2000).
 - [8] W. Shen and S. C. Prager, *Phys. Fluids B* **5**, 1931 (1993).
 - [9] D. L. Brower *et al.*, *Rev. Sci. Instrum.* **74**, 1534 (2003).
 - [10] D. L. Brower *et al.*, *Phys. Rev. Lett.* **88**, 185005 (2002); S. D. Terry *et al.*, *Phys. Plasmas* **11**, 1079 (2004).
 - [11] W. X. Ding *et al.*, *Phys. Rev. Lett.* **90**, 035002 (2003).
 - [12] N. E. Lanier *et al.*, *Phys. Plasmas* **8**, 3402 (2001).
 - [13] H. K. Park, *Plasma Phys. Controlled Fusion* **31**, 2035 (1989).
 - [14] R. J. La Haye *et al.*, *Phys. Fluids* (1958–1988) **27**, 2576 (1984); G. Miller, in Ref. [6], p. 257.